

# Climate change-driven shoreline change along the Catalan coast (NW Mediterranean): A probabilistic approach for risk-informed coastal management

Rut Romero-Martín<sup>a,\*</sup>, Johan Reyns<sup>b,c</sup>, Ali Dastgheib<sup>b,d,e</sup>, Roshanka Ranasinghe<sup>b,c,f</sup>, José A. Jiménez<sup>a</sup>

<sup>a</sup> Laboratori d'Enginyeria Marítima, Universitat Politècnica de Catalunya· BarcelonaTech, c/Jordi Girona 1-3, Campus Nord ed. D1, Barcelona, 08034, Spain

<sup>b</sup> Department of Coastal and Urban Risk & Resilience, IHE Delft Institute for Water Education, Delft, the Netherlands

<sup>c</sup> Resilient Ports and Coasts, Deltares, Delft, the Netherlands

<sup>d</sup> International Marine and Dredging Consultants (IMDC), Van Immerseelstraat 66, 2018, Antwerpen, Belgium

<sup>e</sup> Department of Civil Engineering, Institut Teknologi Sepuluh Nopember, Surabaya, Indonesia

<sup>f</sup> Department of Water Engineering and Management, University of Twente, Enschede, the Netherlands

## ABSTRACT

This study quantifies shoreline retreat for multiple sea-level rise (SLR) projections at two contrasting sites along the Spanish Mediterranean coast: the Llobregat delta and Maresme beaches. The Llobregat delta comprises mildly sloped dissipative beaches, while the Maresme coast is characterized by steeper coarse-sediment beaches. Using the probabilistic PCR model, which incorporates both the effects of the long-term wave climate and Sea level rise, we evaluate site-specific responses and compare outcomes with the widely used Bruun rule. The Bruun rule overestimates retreat by up to 70 % at Llobregat compared to PCR projections under the SSP5-8.5 scenario. At the same time, the results of the two approaches converge at Maresme for both SSPs considered, both at 2050 and 2100. Thus, the discrepancies between the two approaches appear to be larger at sites with milder slopes. The PCR model projects an accelerating retreat from mid-century, reflecting strong nonlinear interactions between future hydrodynamic forcing and storm erosion. These findings underscore the potential pitfalls of relying solely on Bruun rule derived projections for local scale coastal adaptation planning. Moreover, they highlight how PCR model derived physics based, probabilistic projections of shoreline retreat could lead to more informed and effective decisions on local scale adaptation along vulnerable coastlines.

## 1. Introduction

The Mediterranean is recognized as a climate change hotspot experiencing climate change impacts at a rate faster than the global average (MedECC et al., 2024). The high concentration of population, urban development, and infrastructure along the Mediterranean coasts heightens its vulnerability, with risks projected to intensify under the combined effects of climate change and sea-level rise (Burak et al., 2024). Within this regional context, Catalonia, in the northwestern Mediterranean, exemplifies a high-risk area due to both the magnitude of coastal hazards and the intensive development of its shoreline, which has resulted in increasing coastal damage during the last decades (Jiménez et al., 2012). Here, economic activity, population density, and critical infrastructure are concentrated along the coastal zone, severely limiting accommodation space, contributing to positioning Spain among the countries most susceptible to coastal squeeze (Lansu et al., 2024).

This setting, common along much of the European Mediterranean coast, explains why stakeholders identify coastal erosion as one of the most important SLR-induced impacts (Jiménez et al., 2024). Existing studies project substantial beach losses along the Catalan coast by the end of the century (Jiménez et al., 2017), with significant economic implications from reduced recreational carrying capacity (López-Dóriga et al., 2019; Garola et al., 2022), and important consequences for land planning (Romero-Martín et al., 2025).

Although shoreline retreat is widely accepted as a major SLR-induced hazard on sedimentary coasts, its magnitude remains debated due to the lack of a universally accepted predictive model for local scale assessments (Ranasinghe and Stive, 2009; Ranasinghe, 2016; Toimil et al., 2020). Among available approaches, the Bruun Rule is the most commonly applied, largely due to its simplicity and suitability for large-scale assessments (e.g. Hinkel et al., 2013; Vousdoukas et al., 2020; Athanasiou et al., 2020). However, its validity remains contested

\* Corresponding author. Laboratori d'Enginyeria Marítima, Universitat Politècnica de Catalunya· BarcelonaTech, c/Jordi Girona 1-3, Campus Nord ed. D1, Barcelona, 08034, Spain

E-mail address: [rut.romero@upc.edu](mailto:rut.romero@upc.edu) (R. Romero-Martín).

<https://doi.org/10.1016/j.coastaleng.2026.104965>

Received 12 November 2025; Received in revised form 23 January 2026; Accepted 27 January 2026

Available online 27 January 2026

0378-3839/© 2026 The Authors. Published by Elsevier B.V. This is an open access article under the CC BY-NC-ND license (<http://creativecommons.org/licenses/by-nc-nd/4.0/>).

(e.g. Cooper and Pilkey, 2004), and its assumptions restrict the availability of datasets for robust validation (see e.g. Le Cozannet et al., 2016; Zhang et al., 2004). Recent laboratory experiments have attempted to close this gap (e.g. Atkinson et al., 2018; Beuzen et al., 2018; Monioudi et al., 2017), but their number and scope remain limited. In response, alternative or reformulated models have been proposed (e.g. Rosati et al., 2013; Taborda and Ribeiro, 2015) and integrated into broader frameworks that incorporate additional sediment transport processes (e.g. Dean and Houston, 2016; D'Anna et al., 2021; Vitousek et al., 2023).

A key limitation of the Bruun Rule is that the shoreline retreat computed using this method only accounts for the retreat due to SLR alone. Yet storm erosion and incomplete beach recovery can introduce a hysteresis effect that shapes long-term shoreline position and recession (Ranasinghe et al., 2012). Moreover, other ambient local phenomena (e.g. sediment supply from the lower shoreface, fluvial sediment supply to the coast, alongshore gradients in longshore sediment transport) can also contribute to long-term shoreline position change. This combined effect of SLR, wave-driven beach cycles, and ambient processes provides an important framework for isolating the physical impact of climate change on coastal stability in the absence of direct human interventions.

To address this issue, this study applies the Probabilistic Coastline Recession (PCR) model (Ranasinghe et al., 2012). The PCR model incorporates both SLR and storm-driven erosion within a probabilistic, process-based framework that accounts for beach recovery due to ambient processes between storms. The PCR model has been applied globally in different climatic and geomorphic settings (e.g. Wainwright et al., 2015; Jongejan et al., 2016; Le Cozannet et al., 2019; Dastgheib et al., 2018, 2022; Ranasinghe et al., 2023).

In this context, and recognizing the importance of reliable shoreline change projections for effective coastal planning, this study assesses 21st-century coastline evolution in Catalonia using the PCR model under two contrasting SLR projections, corresponding to: low-emission (SSP1-2.6) and a high emission (SSP5-8.5) climate change scenario. To capture regional beach diversity, two representative sites are considered: the Llobregat delta, with dissipative beaches, and the Maresme coast, characterized by coarse-sediment beaches. For comparison, we also estimate SLR-induced shoreline retreat projected by the Bruun rule with identical scenarios and timeframes. This dual assessment enables a comparison between process-based and equilibrium approaches, highlights uncertainty related to model choice, and strengthens the scientific

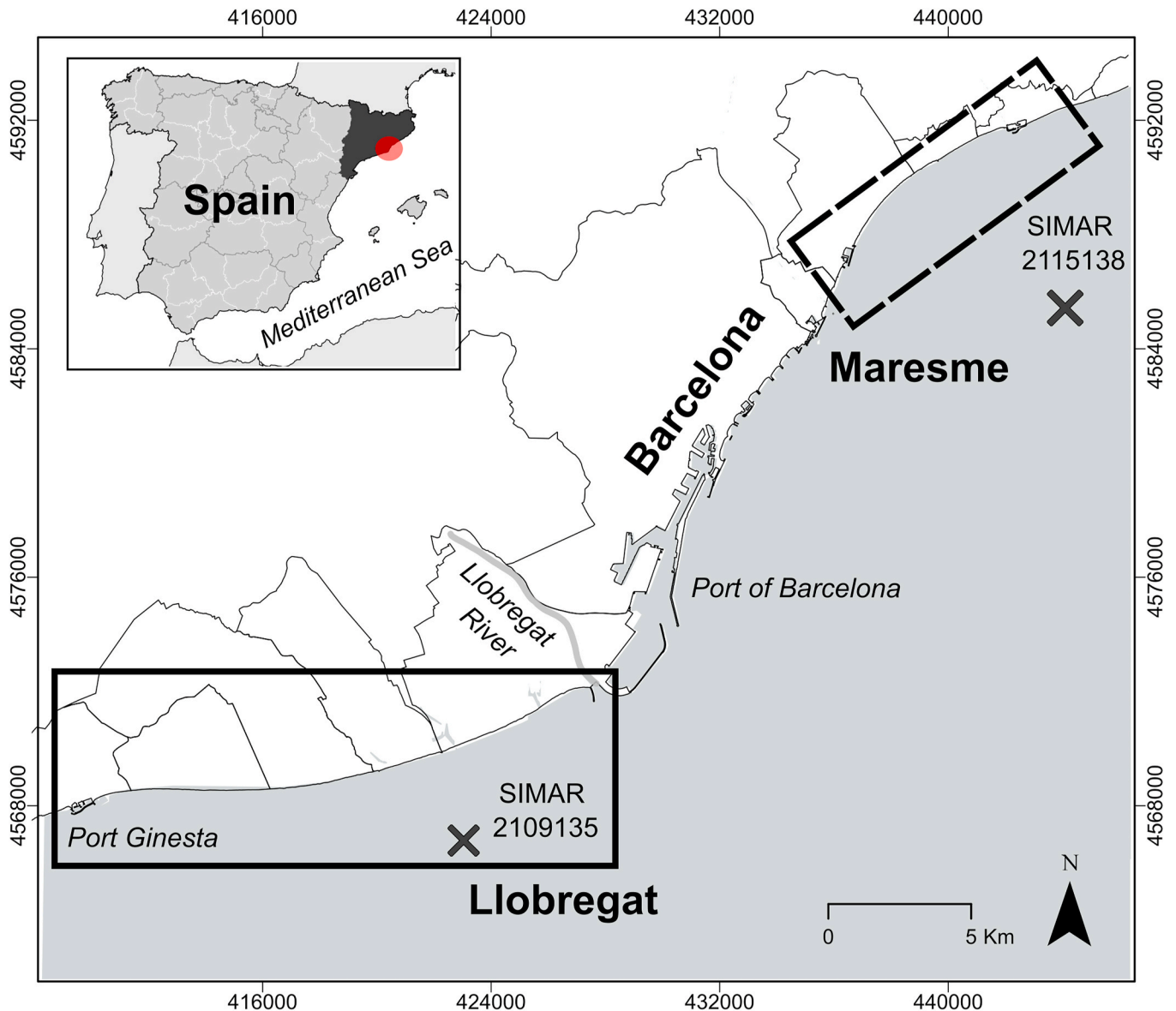


Fig. 1. Study site locations along the Catalan coast: Llobregat and Maresme. The “X” markers indicate the positions of the SIMAR wave nodes used to derive storm wave climates for each site.

basis for adaptation planning in Mediterranean coastal regions.

## 2. Study area and dataset

### 2.1. Study area

The two study sites, Maresme and Llobregat, are located along the Catalan coast (NW Mediterranean), near Barcelona (Fig. 1). These locations were selected to represent contrasting beach morphologies and coastal settings (CIIRC, 2010; Jiménez and Valdemoro, 2019). The Maresme county, situated north of Barcelona, spans approximately 45 km of coastline and is characterized by long, straight, reflective beaches with coarse sediments and steep slopes. The specific study area, located in the southernmost part of Maresme, features a median grain size ( $D_{50}$ ) of 0.63 mm and a beach slope of approximately 1:13. This highly urbanized section of the coast, with an average beach width of 40 m, is backed directly by infrastructure, leaving minimal room for landward beach migration (e.g. Jiménez and Valdemoro, 2019). In contrast, the Llobregat delta, south of Barcelona, comprises an 18 km stretch of deltaic coastline with fine sediment ( $D_{50} = 0.26$  mm) and gently sloping beaches (1:45). Unlike Maresme, this area is backed by a semi-natural landscape, with an average beach width of 100 m, that offers some accommodation space, although key infrastructure and assets are still located close to the shoreline in some spots along the area. Both sites are subject to the bi-directional wave climate typical of the Catalan coast (e.g. Casas-Prat and Sierra, 2012), with offshore dominant waves from NE-E and S sectors. Due to their differing coastline orientations, Maresme is primarily exposed to NE-E storms, whereas Llobregat is more strongly influenced by S-sector storms.

### 2.2. Data

The primary data inputs for the PCR model are SLR projections, beach profile characteristics, storm wave conditions, and water levels. Wave data were obtained from the SIMAR reanalysis dataset (<https://www.puertos.es/es-es>), which provides hourly time series at deep waters. In this work, we have used data from the year 2000 onwards. Specifically, the dataset includes significant wave height ( $H_s$ ), peak wave period ( $T_p$ ), and mean wave direction at two offshore points near the study sites (Fig. 1).

Beach morphology data for both locations were derived from high-resolution topobathymetric surveys conducted in 2022, extending to depths of approximately 15 m (<https://geoportalcartografia.amb.cat/AppGeoportalCartografia2/index.html>). Additionally, monthly time series of shoreline positions were available for both study sites from 2021 to 2023 and were used to assess shoreline behavior under present-day conditions and calibrate beach recovery processes. Both study sites are influenced by longshore sediment transport processes that can induce alongshore-driven shoreline reshaping.

SLR projections used in this study correspond to the median estimates for scenarios SSP1-2.6 and SSP5-8.5 from the IPCC Sixth Assessment Report (AR6, Chapter 9; Fox-Kemper et al., 2021), which have been regionalized for the Barcelona area (Kopp et al., 2023). By 2100, these scenarios project a median SLR value of 0.53 m (SSP1-2.6) and 0.85 m (SSP5-8.5), respectively (Garner et al., 2021).

## 3. Methodology

The probabilistic shoreline projections presented in this study were generated using the PCR model (Ranasinghe et al., 2012), which simulates long-term (i.e., centennial) shoreline change by integrating the combined effects of SLR, storm surge, wave-induced erosion–accretion cycles, and a parameterized aggregation of ambient processes contributing to long-term shoreline position change. The model captures the cumulative impact of erosion from successive storms, superimposed on a gradually rising mean sea level. It also accounts for shoreline recovery

due to integrated ambient processes during inter-storm periods, thereby offering a more realistic representation of coastal morphodynamics over extended timescales. This beach recovery is simulated using an accretion rate that is calibrated through a recovery factor to reproduce observed long-term shoreline trends. This calibration accounts for the aggregated effect of post-storm beach rebuilding due to onshore sediment transport as well as due to ambient processes acting at longer time scales, including sediment supply from the lower shoreface, fluvial inputs, and alongshore gradients in longshore sediment transport (Wainwright et al., 2015; Dastgheib et al., 2018, 2022; Le Cozannet et al., 2019).

In this work, we adopt a two-component modelling framework, as illustrated in Fig. 2: (i) a storm time series generator and (ii) a shoreline changes calculation module. The storm time series generator applies the Joint Probability Method (JPM) (Callaghan et al., 2008) to produce synthetic storm time series spanning approximately 100 years. Each storm is characterized by the significant wave height ( $H_s$ ), peak wave period ( $T_p$ ), and storm duration. These parameters are stochastically generated from extreme value distributions fitted to historical local wave data, allowing the model to represent a broad spectrum of plausible storm events -including rare, high-intensity occurrences-under the assumption that the underlying wave probability density functions remain stationary over time. This hypothesis is consistent with most of the existing wave climate projections in the area under climate change scenarios (e.g. Casas-Prat and Sierra, 2013). To account for dependencies among storm parameters, the relationship between wave height and storm duration is modeled using a Gaussian copula function. Additionally, storm-free intervals (storm gaps) are simulated using a non-homogeneous Poisson distribution following Dastgheib et al. (2018, 2022).

The shoreline evolution module simulates storm-induced erosion and long-term shoreline change. The PCR framework is inherently flexible and has been implemented using different erosion modules depending on local geomorphology and dominant coastal processes (e.g. Callaghan et al., 2013; Dastgheib et al., 2022; Ranasinghe et al., 2023). In this study, we employ the analytical erosion formulation of Mendoza and Jiménez (2006), which has been used in PCR-based assessments at multiple sites (e.g. Dastgheib et al., 2018, 2022; Wang et al., 2024). The model was developed and validated using large-scale experimental beach erosion datasets, together with numerical simulations performed using the SBEACH and XBeach models (Mendoza and Jiménez, 2006; Bosom and Jiménez, 2011; Jiménez et al., 2015). It has also been successfully applied in previous analyses within the present study area (e.g. Jiménez et al., 2018; Romero-Martín et al., 2025). It is worth noting that previous PCR applications further indicate that, while absolute storm-induced erosion magnitudes may vary among erosion formulations, the long-term probabilistic structure of shoreline recession remains relatively robust to the choice of erosion model (Callaghan et al., 2013; Ranasinghe et al., 2023).

The model estimates storm-induced erosion driven by cross-shore sediment transport as a function of storm characteristics ( $H_s$ ,  $T_p$ , storm duration), and beach morphological parameters (beach slope, sediment fall velocity, berm height).

Beach recovery rates during inter-storm periods were calibrated using monthly shoreline position data spanning 2001–2023. For each site, shoreline change increments were computed and their empirical probability distributions derived, which resulted in long-term stability conditions (zero change at 50 % probability level). The recovery rate was then estimated as the value required for the model to reproduce (without SLR) the observed long-term equilibrium shoreline behavior corresponding to the median (50th percentile) response of the cumulative probability distribution. Under present-day conditions, the calibrated recovery rates are 0.013 m/day at Llobregat and 0.014 m/day at Maresme.

Simulations are conducted over a ~100-year period, incorporating a gradually rising mean sea level in accordance with a specified SLR projection. To capture the probabilistic nature of coastal recession, the

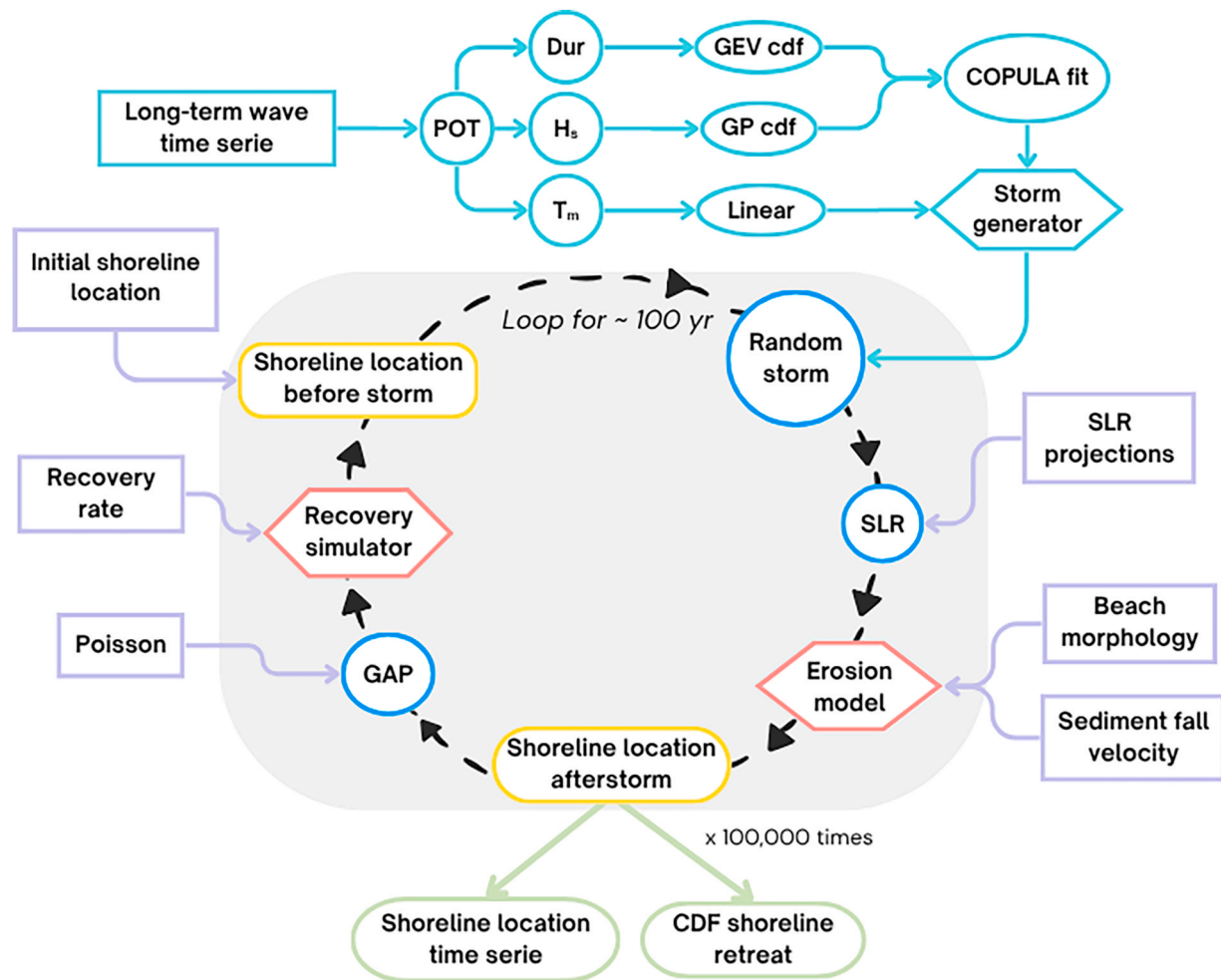


Fig. 2. The conceptual framework of the PCR implementation.

entire process is repeated using a Monte Carlo approach. Simulations are run iteratively until convergence is achieved at low exceedance probabilities (e.g., 0.05). In this study, up to 100,000 iterations were performed to ensure statistical robustness of the results.

For comparative purposes, the Bruun Rule was also applied at the two study sites. Unlike the PCR model, the Bruun rule yields a single deterministic estimate of shoreline retreat based solely on the magnitude of SLR and the active beach profile slope. It assumes a landward and upward translation of the active beach profile in response to SLR, without directly accounting for storm-driven variability or the inherent uncertainty within one SLR projection. Here, we employed the standard Bruun Rule (Bruun, 1962) in which shoreline retreat ( $\Delta X$ ) for a given SLR value ( $s$ ) is expressed as  $\Delta X = s/\tan\beta$ , where  $\tan\beta$  denotes the slope of the active profile (e.g., Le Cozannet et al., 2016; Jiménez et al., 2017; Vousdoukas et al., 2020). To capture potential variability in retreat estimates arising from variability in the shoreface slope, multiple slope measurements were taken across different sections of the study area. This enabled the use of multiple active profile slope values in our Bruun rule calculations, enabling the calculation of a representative median shoreline retreat value, as well as a plausible range of retreat outcomes associated with observed slope variability.

#### 4. Results

Fig. 3 presents the cumulative distribution function (CDF) of PCR-projected shoreline retreat for the years 2050 and 2100 at both study sites. The probability of exceedance reflects the likelihood that the

shoreline will retreat landward by a given distance. Under the baseline scenario without SLR (no-SLR), the median projected shoreline retreat (0.5 exceedance probability) is zero at both locations for both time horizons. However, retreat values increase at lower exceedance probabilities, reflecting the influence of storm-induced erosion. For instance, at the 0.1 exceedance probability level, the projected shoreline retreat reaches 10 m at both sites, Maresme and Llobregat, increasing to approximately 65 m–85 m by 2050 and 2100, respectively.

The inclusion of SLR significantly amplifies projected shoreline retreat across the entire probability spectrum (Fig. 3). Table 1 summarizes the projected shoreline retreats under SSP1-2.6 and SSP5-8.5 for both 2050 and 2100. By 2050, the expected shoreline retreat (0.5 exceedance probability) is similar under both scenarios, as the difference in SLR projections between them remains relatively small at mid-century. Additionally, inter-site differences are minor at this time horizon. Maximum variation in retreat across scenarios at both locations is limited to approximately 20 %, with projected retreat ranging from 12 m to 15 m in Maresme and from 14 m to 17 m in Llobregat. By the end of the century, the influence of scenario variability and inter-site differences becomes more pronounced in absolute terms. Projected shoreline retreat varies by approximately 30 % between SLR projections and by around 20 % between the two sites, with Llobregat exhibiting a larger retreat compared to Maresme (Table 1).

At 0.1 probability of exceedance, projected shoreline retreat increases substantially relative to the median estimates. By 2100, under SSP5-8.5, retreat values are up to 280 % higher in Llobregat and 380 % higher in Maresme compared to the 0.5 exceedance projection (see

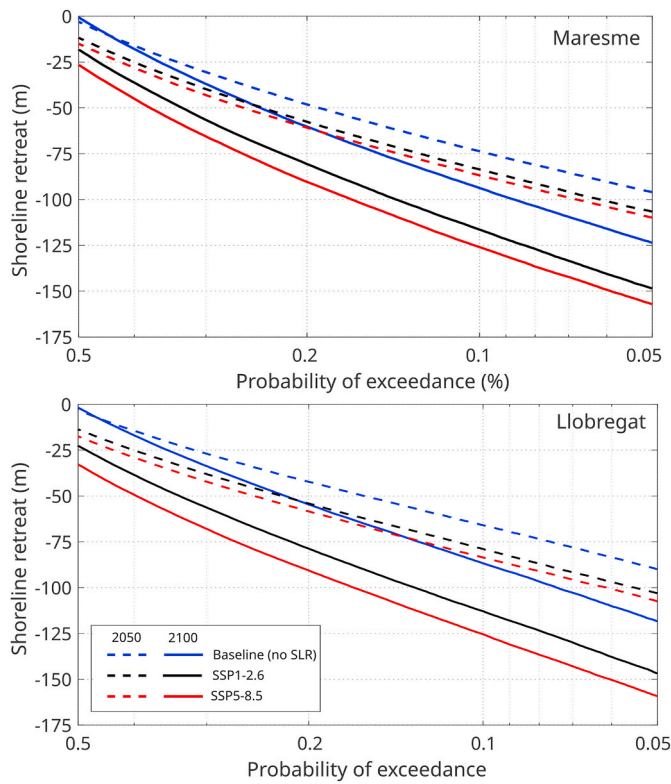


Fig. 3. CDFs of PCR-projected shoreline retreat (negative values) relative to 2023 for 2050 and 2100 under the baseline condition (no SLR), and under SSP1-2.6 and SSP5-8.5. Top: Maresme; bottom: Llobregat.

Table 1

PCR-projected shoreline retreats (negative values) at different exceedance probabilities by mid and end of century under SSP1-2.6 and SSP5-8.5 at Llobregat and Maresme sites.

Prob. of exceedance	Year of projection	Llobregat		Maresme	
		SSP1-2.6	SSP5-8.5	SSP1-2.6	SSP5-8.5
0.5	2050	-14	-17	-12	-15
	2100	-23	-33	-18	-26
0.1	2050	-78	-83	-83	-86
	2100	-112	-125	-116	-125

Table 1).

While the PCR framework is primarily used to project shoreline retreat, it can also be employed to assess the likelihood of complete beach erosion or beach narrowing in areas where rigid structures in the hinterland prevent the natural landward migration and reformation of the beach following shoreline retreat (Nawarat et al., 2024). Although projected shoreline retreat can be assumed relatively uniform along a given coastal segment - provided that local conditions do not significantly alter wave dynamics or beach morphology - the probability of total loss of the emerged beach at a specific location has to be estimated by considering the spatial position of existing inland developments, as they do not necessarily maintain the same alignment along the coast. This spatial variability is illustrated at the Llobregat coastline, which spans approximately 18 km, where inland barriers are located between 30 m and 200 m from the present-day shoreline. As a result, the probability of complete beach loss at this site by 2050 under SSP1-2.6 ranges from 0.36 to 0.007, and from 0.40 to 0.008 under SSP5-8.5. These probabilities increase substantially by 2100, reaching maximum values of 0.45 and 0.51, under SSP1-2.6 and SSP5-8.5, respectively.

While the standard application of the PCR model accounts for

shoreline retreat driven by the combined effects of SLR and wave climate (Fig. 3), it is also insightful to isolate and assess the specific contribution of SLR to the projected retreat. This is done here by subtracting the retreat projected under baseline scenario (i.e., storms only, no SLR) from the PCR-projected retreat under each SLR projection (with storms and SLR non-linearly acting together) at specific time horizons (2050 and 2100), following the approach taken by Ranasinghe et al. (2023). Fig. 4 presents the SLR-induced component of shoreline retreat (for a range of exceedance probabilities), in the absence of any physical obstruction to shoreline retreat, computed in this way at the Llobregat and Maresme sites throughout the 21st century, under SSP1-2.6 and SSP5-8.5. Results reveal a consistent temporal pattern across exceedance probabilities at both locations. Until around 2040, SLR-induced retreat is similar under both scenarios for all exceedance probabilities considered. However, in the latter half of the century, the SLR-induced retreat increases (all considered exceedance probabilities) sharply under SSP5-8.5, diverging from the more gradual trend projected under SSP1-2.6. By 2100, SLR-driven retreat is approximately 50 % greater with SSP5-8.5 compared to SSP1-2.6 at both sites (see Table 2). The magnitude of the SLR-induced retreat is about 20 % higher in Llobregat compared to Maresme under both scenarios by the end of the century (Table 2).

Once the median (0.5 exceedance probability) SLR-induced component is isolated from the PCR response, it can be compared with estimates derived using the Bruun rule, as shown in Fig. 4. The temporal evolution of shoreline retreat follows a similar trend across both methods: projections under SSP1-2.6 and SSP5-8.5 remain comparable until around 2040, after which retreat increases substantially under SSP5-8.5 in the second half of the century. The Bruun rule produces significantly different retreat estimates at the two study sites, as its results have a linear relationship with the slope of the active profile, which varies with local beach morphology. Specifically, the average slope in

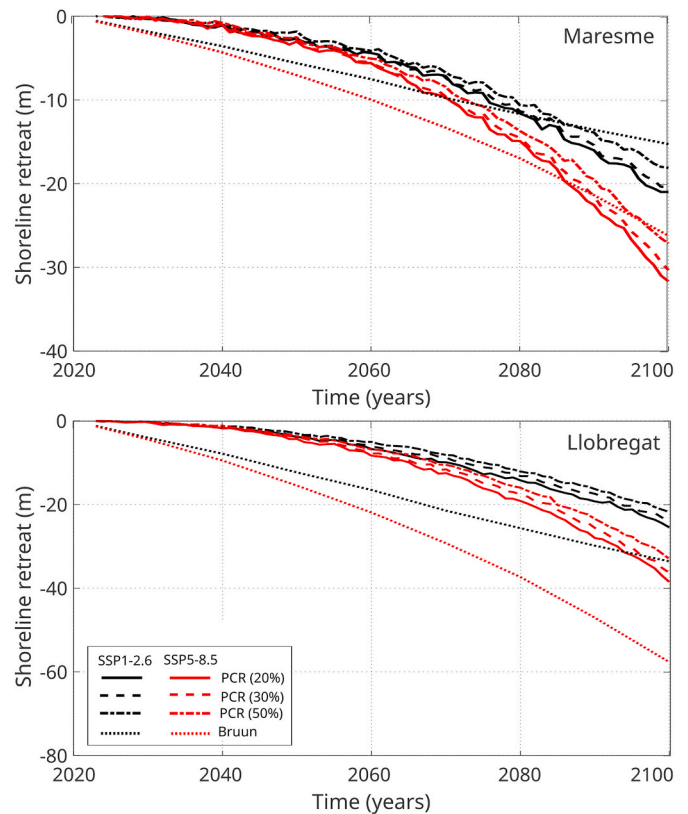


Fig. 4. PCR model projections of SLR-driven shoreline retreat (negative values) across the 21st century (relative to 2023) under SSP1-2.6 and SSP5-8.5, and comparable Bruun rule derived shoreline retreat projections. Top: Maresme; bottom: Llobregat.

**Table 2**

SLR-driven shoreline retreats (negative values) projected by the PCR model and the Bruun Rule at Maresme and Llobregat study sites by 2050 and 2100 relative to 2023 under SSP1-2.6 and SSP5-8.5 scenarios.

Site	scenario	Bruun		PCR (median)	
		2050	2100	2050	2100
Maresme	SSP1-2.6	-5	-15	-2	-18
	SSP5-8.5	-7	-26	-2.5	-27
Llobregat	SSP1-2.6	-12	-33	-3	-22
	SSP5-8.5	-15	-56	-4	-33

Maresme (0.0294) is approximately twice as steep as that in Llobregat (0.0134), resulting in Bruun-derived shoreline retreats in Llobregat that are roughly double those in Maresme. In contrast, this direct inverse relationship between slope and retreat is not evident in the SLR-driven component of the PCR projections, leading to notable discrepancies between the two approaches. By 2100, both the PCR and Bruun rule produce shoreline retreats of similar magnitude in Maresme under both SLR projections (Fig. 4 and Table 2). However, at Llobregat, the Bruun rule projects retreat values approximately 70 % higher under SSP5-8.5, and 50 % higher under SSP1-2.6, compared to median projections from the PCR model (Fig. 4 and Table 2).

By mid-century, the Bruun rule consistently predicts greater shoreline retreat than the median projections of the PCR model at both sites and under both scenarios. This difference stems from how each model relates shoreline retreat to SLR. Fig. 5 illustrates the relationship between average shoreline retreat rates and SLR rates, calculated per decade over the study period. Under SSP1-2.6, the Bruun-derived retreat rate remains constant through the period, reflecting the nearly linear increase in SLR (i.e., a constant rate of SLR). Since the Bruun rule links retreat only to profile slope and SLR rate, the result is a uniform retreat rate (so a single value in Fig. 5 subplots – filled black circle). In contrast, the PCR model predicts varying retreat rates over time, highlighting the cumulative effects of beach erosion even when the SLR rate is steady. For scenario SSP5-8.5, the Bruun rule produces a linearly increasing retreat rate, mirroring the accelerating SLR. However, the PCR model predicts a non-linear increase in retreat, again emphasizing the cumulative impact of beach profile erosion, particularly pronounced after 2055. In essence, while the Bruun rule treats shoreline retreat as a linear function of SLR, the PCR model captures the non-linear relationship between forcing and

response where coastal erosion is concerned, as illustrated by the projected acceleration in retreat even without concurrent increases in SLR rates (e.g., in SSP1-2.6).

## 5. Discussion and conclusions

This study presents a detailed analysis of shoreline retreat projections for multiple SLR projections using the probabilistic PCR model at two contrasting locations along the Spanish Mediterranean coast: Llobregat and Maresme. These locations differ notably in sediment grain size, shoreface slopes, and wave climate. By applying the PCR model, we evaluate how site-specific conditions influence beach evolution under each SLR projection. This approach offers a more nuanced alternative to the conceptually simpler yet widely used Bruun rule, which considers only active profile slope and local SLR rates. Additionally, the integration of long-term wave climate data within a probabilistic approach is essential for effective coastal risk management. This methodology enables the estimation of shoreline retreat across different probabilities of occurrence, providing decision-makers with valuable insights for setting appropriate safety thresholds.

While the current PCR implementation assesses shoreline retreat and recovery using independent estimates for storm and post-storm periods, thus preserving their statistical representation within the wave climate, a promising alternative would be the integration of multi-temporal shoreline evolution models (e.g., Davidson et al., 2017; Montaña et al., 2020). Such models would allow the explicit representation of processes including storm clustering, beach memory, and post-storm beach recovery, leading to a more physics based representation of coastal response. To remain consistent with the probabilistic nature of the PCR framework, these models would need to be driven by multiple realizations of the wave climate under per climate scenarios in order to capture natural variability and associated uncertainty (e.g., Toimil et al., 2021; D'Anna et al., 2022). However, their application also raises the unresolved issue of how SLR influences shoreline erosion-recovery dynamics, as most multi-temporal evolution models parameterize shoreline change primarily as a function of incident wave conditions, without explicitly accounting for variations in mean sea level. In practice, this limitation is often addressed by incorporating a long-term SLR-related component based on the Bruun rule (e.g., Dean and Houston, 2016; Toimil et al., 2017; Vitousek et al., 2017). While this approach provides a pragmatic solution, it implicitly assumes the validity of the Bruun

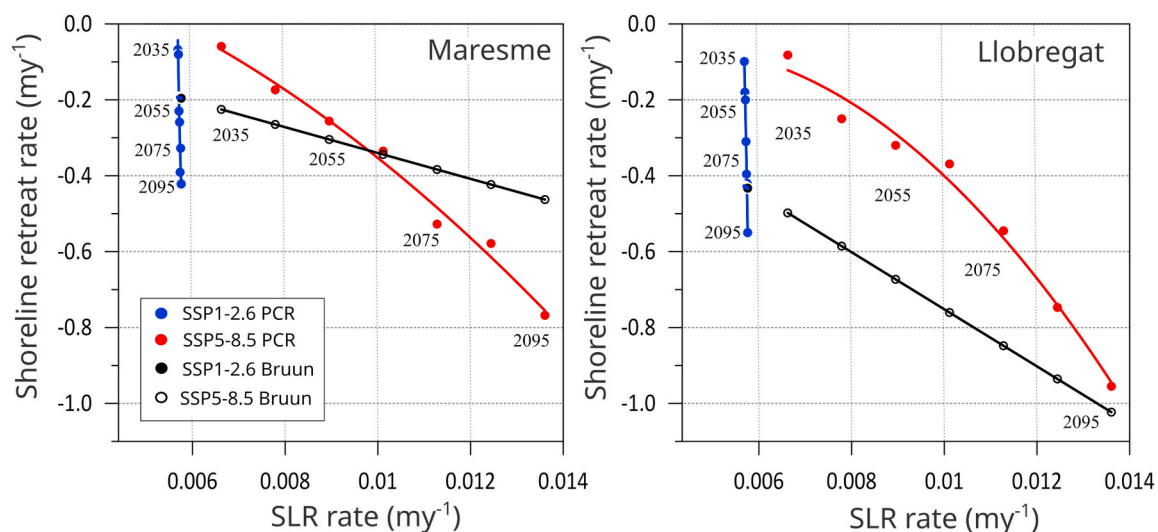


**Fig. 5.** Median shoreline retreat rates calculated by the PCR model and Bruun rule-derived projections for different SLR rates over the study period for the SSP1-2.6 and SSP5-8.5 at Maresme (left) and Llobregat (right). Each data point represents a 10-year average, with dates indicating the center of the relevant 10-year interval. Solid lines indicate the best-fit relationships for each dataset, while the red dashed line represents the best linear fit to SSP5-8.5 PCR projection up to mid-century SLR rates.

formulation and thus reintroduces the same conceptual limitations that motivate the development of alternative modelling approaches such as PCR, which completely departs from the Bruun Rule.

Despite their differing conceptual frameworks, the PCR model and Bruun rule derived projections exhibit broadly similar patterns: the location with the gentler active beach profile is projected to experience greater long-term retreat in response to the same SLR than that with the site with steeper one. However, the magnitude of the projected retreat varies notably between the two approaches, with larger discrepancies occurring at sites with milder slopes. At the Llobregat delta, for instance, the Bruun rule predicts shoreline retreats up to 70 % greater compared to the median projection from the PCR model under SSP5-8.5. In contrast, at Maresme, both models yield comparable retreat projections by the end of the century. These results are consistent with previous findings on the divergence between the two approaches (Ranasinghe et al., 2012; Dastgheib et al., 2018), and highlight that discrepancies in projections are not uniform across settings. This underscores the importance of extending model comparisons to a wider range of coastal environments to enhance generalizability.

It is important to note that the differences between the PCR and Bruun rule derived projections exhibit distinct temporal patterns throughout the study period. While shoreline retreats projected by the Bruun rule increases linearly with SLR, the PCR projections progressively incorporates the compounding effects of SLR and storms, simulating the enhanced beach erosion associated with rising water levels. This cumulative erosion response becomes evident at both sites by mid-century (2050), when retreat projections under SSP5-8.5 begin to increase at a faster rate than SLR itself, indicating that shoreline retreat accelerates disproportionately with continued SLR. This inflection at the mid-21st century may be interpreted as a tipping point, which could be defined as a critical threshold where small changes in external forcing trigger a nonlinear system response. Identifying the timing of such accelerated shoreline change is crucial for informing timely adaptation strategies, particularly in areas where the current shoreline lies in proximity to inland developments. In these cases, the risk of beach narrowing and increased exposure of the hinterland to storm impacts may grow substantially and fast, leading to increased coastal damage (e.g., Jiménez et al., 2012). It is noteworthy that previous studies examining the impact of SLR across various coastal environments (e.g., Barnard et al., 2011; Wang et al., 2024) have identified the onset of tipping points at broadly similar times. These typically correspond to an SLR of approximately 0.25 m, regardless of the specific scenario considered.

It is important to note that the nonlinear response identified here arises solely from the cumulative effects of SLR on beach erosion, as the analysis assumes a stationary incident wave climate, an assumption consistent with existing wave climate projections for the study area. While this approach isolates the contribution of SLR, future changes in wave parameters may influence shoreline evolution (Casas-Prat and Sierra, 2013; Lira-Loarca and Besio, 2022).

Finally, this study provides valuable insights into the projected evolution of the Catalan coastline under different SLR projections. It aligns with previous estimates of areas most susceptible to SLR-induced retreat (Jiménez et al., 2017) while highlighting the limitations of relying solely on the Bruun rule for informing risk management. The probabilistic shoreline-retreat estimates presented in this study provide a framework that can be directly applied to coastal risk assessments and risk-informed adaptation planning under SLR. In Mediterranean settings, where setback zones are increasingly promoted in line with the ICZM Protocol for the in the Mediterranean (UNEP/MAP/PAP, 2008; Sanò et al., 2011), exceedance-based retreat projections offer a risk-informed basis for defining buffer widths and adaptive zoning that reflect different levels of acceptable risk over specified planning horizons. By framing setback lines as probabilistic, rather than deterministic, planning instruments, this approach is particularly suited to erosion-prone and highly developed coastlines, where uniform buffers are often difficult to justify economically, socially, politically or

environmentally (e.g. Wainwright et al., 2015).

The time-dependent trajectories generated by the PCR framework further align with dynamic adaptation-pathway approaches (e.g. Haasnoot et al., 2019) by enabling the identification of probability (or risk)-based trigger points and decision windows for intervention. This supports the sequencing and timing of adaptation measures, such as transitioning from beach nourishment or hybrid protection strategies toward managed retreat once the likelihood of exceeding critical retreat thresholds, or the estimated annual damage (risk) becomes unacceptable under a given SLR scenario (Haasnoot et al., 2021).

Beyond supporting technical decision-making, the explicit use of exceedance probabilities, or risk estimates, enhances the transparency, credibility, and defensibility of adaptation strategies (Desai et al., 2021). This is especially relevant in Mediterranean coastal contexts, where shoreline erosion interacts with dense development, tourism-dependent economies, and socially sensitive relocation processes, and where clear, defensible risk information is essential for long-term planning and stakeholder acceptance.

### 5.1. Limitations

One of the main challenges in the PCR model is accurately simulating shoreline erosion-accretion cycles and assessing how these processes are influenced by SLR. In the absence of a universally validated erosion model, the bulk erosion model proposed by Mendoza and Jiménez (2006) has been employed. This model is computationally efficient for probabilistic modelling involving hundreds of thousands of individual simulations, as required in this study. Although originally developed for the Spanish Mediterranean coast, it has been successfully applied in other settings (e.g. Armaroli and Duo, 2018; Dastgheib et al., 2018, 2022). While alternative erosion models might yield different shoreline retreat estimates, the probabilistic framework of the PCR model helps mitigate some of the associated uncertainties. However, the simplicity of the chosen erosion model limits its ability to capture complex cross-shore sediment transport dynamics and other non-linear processes. Future research should therefore assess the sensitivity of PCR outcomes to different erosion models, particularly given the lack of a widely accepted standard (Ranasinghe, 2020; Toimil et al., 2020; Sherwood et al., 2022).

Another key source of uncertainty is the impact of SLR on post-storm beach recovery, which is taken as a proxy for the aggregated effect of shoreline position change due to ambient processes. Most PCR model applications assume constant beach recovery during inter-storm periods (Wainwright et al., 2015; Dastgheib et al., 2018, 2022; Le Cozannet et al., 2019), reflecting the current limited understanding of, among others, how SLR may influence cross-shore sediment exchanges between the upper and lower shorefaces. In this context, several studies (e.g., Stive and De Vriend, 1995; Anthony and Aagaard, 2020) suggest that rising sea levels may reduce sediment supply from the lower shoreface to the active beach profile. This diminished recovery capacity could lead to a progressive imbalance in the sediment budget. Such imbalances may either be compensated for or exacerbated by variations in fluvial sediment supply and sedimentation or erosion driven by changes in along-shore gradients in longshore sediment transport.

### CRediT authorship contribution statement

**Rut Romero-Martín:** Writing – review & editing, Writing – original draft, Visualization, Software, Methodology, Investigation, Formal analysis, Data curation. **Johan Reyns:** Writing – review & editing, Software. **Ali Dastgheib:** Writing – review & editing. **Roshanka Ranasinghe:** Writing – review & editing, Supervision, Methodology, Conceptualization. **José A. Jiménez:** Writing – review & editing, Writing – original draft, Supervision, Project administration, Funding acquisition, Conceptualization.

## Declaration of competing interest

The authors declare that they have no known competing financial interests or personal relationships that could have appeared to influence the work reported in this paper.

## Acknowledgements

This work has been done in the framework of the CoastSpace research project (TED2021-130001B-C21) funded by MCIN/AEI/10.13039/501100011033 and by the European Union “NextGenerationEU”/PRTR. We thank Puertos del Estado for access to wave data and the Autoritat Metropolitana de Barcelona (AMB) for access to morphological data at both study sites. The first author was funded by a PhD Grant from the Ministry of Science and Innovation (PRE2018-084174). JAJ acknowledges the support of the Departament de Recerca i Universitats of the Generalitat de Catalunya (Acadèmia d'Excel·lència award).

## Data availability

Data will be made available on request.

## References

- Anthony, E.J., Aagaard, T., 2020. The lower shoreface: morphodynamics and sediment connectivity with the upper shoreface and beach. *Earth Sci. Rev.* 210, 103334. <https://doi.org/10.1016/j.earscirev.2020.103334>.
- Armaroli, C., Duo, E., 2018. Validation of the coastal storm risk assessment framework along the Emilia-Romagna coast. *Coast. Eng.* 134, 159–167. <https://doi.org/10.1016/j.coastaleng.2017.08.014>.
- Athanasios, P., van Dongeren, A., Giardino, A., Voudoukas, M.I., Ranasinghe, R., Kwadijk, J., 2020. Uncertainties in projections of sandy beach erosion due to sea level rise: an analysis at the European scale. *Sci. Rep.* 10, 11895. <https://doi.org/10.1038/s41598-020-68576-0>.
- Atkinson, A.L., Baldock, T.E., Birrien, F., Callaghan, D.P., Nielsen, P., Beuzen, T., Turner, I.L., Blenkinsopp, C.F., Ranasinghe, R., 2018. Laboratory investigation of the Bruun rule and beach response to sea level rise. *Coast. Eng.* 136, 183–202. <https://doi.org/10.1016/j.coastaleng.2018.03.003>.
- Barnard, P.L., Allan, J., Hansen, J.E., Kaminsky, G.M., Ruggiero, P., Doria, A., 2011. The impact of the 2009–10 El Niño Modoki on US west coast beaches. *Geophys. Res. Lett.* 38, L13604. <https://doi.org/10.1029/2011GL047707>.
- Beuzen, T., Turner, I.L., Blenkinsopp, C.E., Atkinson, A., Flocard, F., Baldock, T.E., 2018. Physical model study of beach profile evolution by sea level rise in the presence of seawalls. *Coast. Eng.* 136, 172–182. <https://doi.org/10.1016/j.coastaleng.2017.12.002>.
- Bosom, E., Jiménez, J.A., 2011. Probabilistic coastal vulnerability assessment to storms at regional scale-application to Catalan beaches (NW Mediterranean). *Nat. Hazards Earth Syst. Sci.* 11, 475–484. <https://doi.org/10.5194/nhess-11-475-2011>.
- Bruun, P., 1962. Sea-level rise as a cause of shore erosion. *J. Waterw. Harb. Div.* 88, 117–130. <https://doi.org/10.1061/JWHEAU.0000252>.
- Burak, Z.S., Hilmi, N., Jiménez, J.A., et al., 2024. Impacts and risks. In: Djoundourian, S., Lionello, P., Llasat, M.C., Guiot, J., Cramer, W., Driouech, F., Gattacceca, J.C., Marini, K. (Eds.), *Climate and Environmental Coastal Risks in the Mediterranean*, MedECC Secretariat, Marseille, France, pp. 131–208. <https://doi.org/10.5281/zenodo.15096247>.
- Callaghan, D.P., Ranasinghe, R., Roelvink, D., 2013. Probabilistic estimation of storm erosion using analytical, semi-empirical, and process based storm erosion models. *Coast. Eng.* 82, 64–75. <https://doi.org/10.1016/j.coastaleng.2013.08.007>.
- Callaghan, D.P., Nielsen, P., Short, A., Ranasinghe, R., 2008. Statistical simulation of wave climate and extreme beach erosion. *Coast. Eng.* 55, 375–390. <https://doi.org/10.1016/j.coastaleng.2007.12.003>.
- Casas-Prat, M., Sierra, J.P., 2013. Projected future wave climate in the NW Mediterranean Sea. *J. Geophys. Res., Oceans* 118, 3548–3568. <https://doi.org/10.1002/jgrc.20233>.
- Casas-Prat, M., Sierra, J.P., 2012. Trend analysis of wave direction and associated impacts on the Catalan coast. *Clim. Change* 115, 667–691. <https://doi.org/10.1007/s10584-012-0466-9>.
- CIIRC, 2010. *Estat De La Zona Costanera a Catalunya*. International Centre for Coastal Resources Research, Barcelona, p. 25. Resum executiu. <https://icgc.cat/Administracio-i-empresa/Serveis/Riscos-geologics/Dinamica-de-la-costa/Llibre-verd-de-l-Estat-de-la-zona-costanera-a-Catalunya-2010/Llibre-verd-de-l-Estat-de-la-zona-costanera-a-Catalunya-2010>.
- Cooper, J.A.G., Pilkey, O.H., 2004. Sea-level rise and shoreline retreat: time to abandon the Bruun rule. *Global Planet. Change* 43, 157–171. <https://doi.org/10.1016/j.gloplacha.2004.07.001>.
- D'Anna, M., Idier, D., Castelle, B., Vitousek, S., Le Cozannet, G., 2021. Reinterpreting the Bruun rule in the context of equilibrium shoreline models. *J. Mar. Sci. Eng.* 9, 974. <https://doi.org/10.3390/jmse9090974>.
- D'Anna, M., Idier, D., Castelle, B., Rohmer, J., Cagigal, L., Mendez, F.J., 2022. Effects of stochastic wave forcing on probabilistic equilibrium shoreline response across the 21st century including sea-level rise. *Coast. Eng.* 175, 104149. <https://doi.org/10.1016/j.coastaleng.2022.104149>.
- Dastgheib, A., Jongejan, R., Wickramanayake, M., Ranasinghe, R., 2018. Regional scale risk-informed land-use planning using probabilistic coastline recession modelling and economical optimisation: east coast of Sri Lanka. *J. Mar. Sci. Eng.* 6, 120. <https://doi.org/10.3390/jmse6040120>.
- Dastgheib, A., Martínez, C., Udo, K., Ranasinghe, R., 2022. Climate change driven shoreline change at Hasaki beach Japan: a novel application of the probabilistic coastline recession (PCR) model. *Coast. Eng.* 172, 104079. <https://doi.org/10.1016/j.coastaleng.2021.104079>.
- Davidson, M.A., Turner, I.L., Splinter, K.D., Harley, M.D., 2017. Annual prediction of shoreline erosion and subsequent recovery. *Coast. Eng.* 130, 14–25. <https://doi.org/10.1016/j.coastaleng.2017.09.008>.
- Dean, R.G., Houston, J.R., 2016. Determining shoreline response to sea level rise. *Coast. Eng.* 114, 1–8. <https://doi.org/10.1016/j.coastaleng.2016.03.009>.
- Desai, B., Bresch, D.N., Cazabat, C., Hochrainer-Stigler, S., Mechler, R., Ponserrre, S., Schewe, J., 2021. Addressing the human cost in a changing climate. *Science* 372 (6548), 1284–1287. <https://doi.org/10.1126/science.abb4283>.
- Fox-Kemper, B., Hewitt, H.T., Xiao, C., et al., 2021. Ocean, cryosphere and sea level change. In: Masson-Delmotte, V., Zhai, P., Pirani, A., et al. (Eds.), *Climate Change 2021: the Physical Science Basis*. Contribution of Working Group I to the Sixth Assessment Report of the Intergovernmental Panel on Climate Change. Cambridge University Press, Cambridge, pp. 1211–1362. <https://doi.org/10.1017/9781009157896.011>.
- Garner, G., Hermans, T.H., Kopp, R., et al., 2021. IPCC AR6 WGI sea level projections. Version 20210809. <https://doi.org/10.5281/zenodo.5914709>. Dataset accessed [2025-03-10] at.
- Garola, A., López-Dóriga, U., Jiménez, J.A., 2022. The economic impact of sea level rise-induced decrease in the carrying capacity of Catalan beaches (NW Mediterranean, Spain). *Ocean Coast. Manag.* 218, 106034. <https://doi.org/10.1016/j.ocecoaman.2022.106034>.
- Haasnoot, M., Lawrence, J., Magnan, A.K., 2021. Pathways to coastal retreat. *Science* 373 (6548), 1287–1290. <https://doi.org/10.1126/science.abi6594>.
- Haasnoot, M., Brown, S., Scussolini, P., Jiménez, J.A., Vafeidis, A., Nicholls, R.J., 2019. Generic adaptation pathways for coastal archetypes under uncertain sea-level rise. *Environ. Res. Commun.* 1 (7), 071006. <https://doi.org/10.1088/2515-7620/ab1871>.
- Hinkel, J., Nicholls, R.J., Tol, R.S., et al., 2013. A global analysis of erosion of sandy beaches and sea-level rise: an application of DIVA. *Global Planet. Change* 111, 150–158. <https://doi.org/10.1016/j.gloplacha.2013.09.002>.
- Jiménez, J.A., Valdemoro, H.I., 2019. Shoreline evolution and its management implications in beaches along the Catalan coast. *The Spanish Coastal Systems: Dynamic Processes. Sediments and Management*, pp. 745–764. [https://doi.org/10.1007/978-3-319-93169-2\\_32](https://doi.org/10.1007/978-3-319-93169-2_32).
- Jiménez, J.A., Sanuy, M., Ballesteros, C., Valdemoro, H.I., 2018. The Tordera Delta, a hotspot to storm impacts in the coast northwards of Barcelona (NW Mediterranean). *Coast. Eng.* 134, 148–158. <https://doi.org/10.1016/j.coastaleng.2017.08.012>.
- Jiménez, J.A., Sancho-García, A., Bosom, E., Valdemoro, H.I., Guillén, J., 2012. Storm-induced damages along the Catalan coast (NW Mediterranean) during the period 1958–2008. *Geomorphology* 143, 24–33. <https://doi.org/10.1016/j.geomorph.2011.07.034>.
- Jiménez, J.A., Valdemoro, H.I., Bosom, E., S-Arcilla, A., Nicholls, R.J., 2017. Impacts of sea-level rise-induced erosion on the Catalan coast. *Reg. Environ. Change* 17, 593–603. <https://doi.org/10.1007/s10113-016-1052-x>.
- Jiménez, J.A., Armaroli, C., Berenguer, M., et al., 2015. *Coastal Hazard Assessment Module*. RISC-KIT D, 2.1.
- Jiménez, J.A., Bonaduce, A., Depuydt, M., et al., 2024. Sea Level rise in Europe: knowledge gaps identified through a participatory approach. *State of the Planet*, 3-slre1 3. <https://doi.org/10.5194/sp-3-slre1-3-2024>.
- Jongejan, R., Ranasinghe, R., Wainwright, D., Callaghan, D.P., Reyns, J., 2016. Drawing the line on coastline recession risk. *Ocean Coast Manag.* 122, 87–94. <https://doi.org/10.1016/j.ocecoaman.2016.01.006>.
- Kopp, R.E., Garner, G.G., Hermans, T.H.J., et al., 2023. The framework for assessing changes to sea-level (FACTS) v1.0: a platform for characterizing parametric and structural uncertainty in future global, relative, and extreme sea-level change. *Geosci. Model Dev. (GMD)* 16, 7461–7489. <https://doi.org/10.5194/gmd-16-7461-2023>.
- Lansu, E.M., Reijers, V.C., Höfer, S., et al., 2024. A global analysis of how human infrastructure squeezes sandy coasts. *Nat. Commun.* 15, 432. <https://doi.org/10.1038/s41467-023-44659-0>.
- Le Cozannet, G., Bulteau, T., Castelle, B., et al., 2019. Quantifying uncertainties of sandy shoreline change projections as sea level rises. *Sci. Rep.* 9, 42. <https://doi.org/10.1038/s41598-018-37017-4>.
- Le Cozannet, G., Oliveros, C., Castelle, B., Garcin, M., Idier, D., Pedreros, R., Rohmer, J., 2016. Uncertainties in sandy shorelines evolution under the Bruun rule assumption. *Front. Mar. Sci.* 3, 49. <https://doi.org/10.3389/fmars.2016.00049>.
- Lira-Loarca, A., Besio, G., 2022. Future changes and seasonal variability of the directional wave spectra in the Mediterranean Sea for the 21st century. *Environ. Res. Lett.* 17, 104015. <https://doi.org/10.1088/1748-9326/ac8ec4>.

- López-Dóriga, U., Jiménez, J.A., Valdemoro, H.I., Nicholls, R.J., 2019. Impact of sea-level rise on the tourist-carrying capacity of Catalan beaches. *Ocean Coast Manag.* 170, 40–50. <https://doi.org/10.1016/j.ocecoaman.2018.12.028>.
- MedECC, 2024. Climate and environmental coastal risks in the mediterranean. In: Djoundourian, S., Lionello, P., Llasat, M.C., Guiot, J., Cramer, W., Driouech, F., Gattacceca, J.C., Marini, K. (Eds.), *MedECC Secretariat*, Marseille, France, p. 306. <https://doi.org/10.5281/zenodo.13754020>.
- Mendoza, E.T., Jiménez, J.A., 2006. Storm-induced beach erosion potential on the catalonian coast. *J. Coast. Res.* SI 48, 81–88. [https://doi.org/10.1061/40855\(214\)98](https://doi.org/10.1061/40855(214)98).
- Monioudi, I.N., Velegrakis, A.F., Chatzipavlis, A.E., et al., 2017. Assessment of island beach erosion due to sea level rise: the case of the Aegean archipelago (Eastern mediterranean). *Nat. Hazards Earth Syst. Sci.* 17, 449–466. <https://doi.org/10.5194/nhess-17-449-2017>.
- Montaño, J., Coco, G., Antolínez, J.A.A., Beuzen, T., Bryan, K.R., Cagigal, L., et al., 2020. Blind testing of shoreline evolution models. *Sci. Rep.* 10, 2137. <https://doi.org/10.1038/s41598-020-59018-y>.
- Nawarat, K., Reyns, J., Voudoukas, M.I., Duong, T.M., Kras, E., Ranasinghe, R., 2024. Coastal hardening and what it means for the world's sandy beaches. *Nat. Commun.* 15, 10626. <https://doi.org/10.1038/s41467-024-54952-1>.
- Ranasinghe, R., 2016. Assessing climate change impacts on open sandy coasts: a review. *Earth Sci. Rev.* 160, 320–332. <https://doi.org/10.1016/j.earscirev.2016.07.011>.
- Ranasinghe, R., Stive, M.J.F., 2009. Rising seas and retreating coastlines. *Clim. Change* 97, 465–468. <https://doi.org/10.1007/s10584-009-9593-3>.
- Ranasinghe, R., Callaghan, D., Stive, M.J.F., 2012. Estimating coastal recession due to sea level rise: beyond the Bruun rule. *Clim. Change* 110, 561–574. <https://doi.org/10.1007/s10584-011-0107-8>.
- Ranasinghe, R., 2020. On the need for a new generation of coastal change models for the 21<sup>st</sup> century. *Sci Rep* 10, 2010. <https://doi.org/10.1038/s41598-020-58376-x>.
- Ranasinghe, R., Callaghan, D.P., Li, F., Wainwright, D.J., Duong, T.M., 2023. Assessing coastline recession for adaptation planning: sea level rise versus storm erosion. *Sci. Rep.* 13, 8286. <https://doi.org/10.1016/j.coastaleng.2007.12.003>.
- Romero-Martín, R., Valdemoro, H.I., Jiménez, J.A., 2025. Unveiling coastal adaptation demands: exploring erosion-induced spatial imperatives on the Catalan Coast (NW Mediterranean). *Landsc. Urban Plann.* 263, 105450. <https://doi.org/10.1016/j.landurbplan.2025.105450>.
- Rosati, J.D., Dean, R.G., Walton, T.L., 2013. The modified Bruun rule extended for landward transport. *Mar. Geol.* 340, 71–81. <https://doi.org/10.1016/j.margeo.2013.04.018>.
- Sanò, M., Jiménez, J.A., Medina, R., Stanica, A., S-Arcilla, A., Trumbic, I., 2011. The role of coastal setbacks in the context of coastal erosion and climate change. *Ocean Coast Manag.* 54, 943–950. <https://doi.org/10.1016/j.ocecoaman.2011.06.008>.
- Sherwood, C.R., Van Dongeren, A., Doyle, J., et al., 2022. Modeling the morphodynamics of coastal responses to extreme events: what shape are we in? *Ann. Rev. Mar. Sci.* 14, 457–492. <https://doi.org/10.1146/annurev-marine-032221-090215>.
- Stive, M.J., De Vriend, H.J., 1995. Modelling shoreface profile evolution. *Mar. Geol.* 126 (1–4), 235–248.
- Taborda, R., Ribeiro, M.A., 2015. A simple model to estimate the impact of sea-level rise on platform beaches. *Geomorphology* 234, 204–210. <https://doi.org/10.1016/j.geomorph.2015.01.015>.
- Toimil, A., Camus, P., Losada, I.J., Alvarez-Cuesta, M., 2021. Visualising the uncertainty cascade in multi-ensemble probabilistic coastal erosion projections. *Front. Mar. Sci.* 8, 683535. <https://doi.org/10.3389/fmars.2021.683535>.
- Toimil, A., Losada, I.J., Camus, P., Diaz-Simal, P., 2017. Managing coastal erosion under climate change at the regional scale. *Coast. Eng.* 128, 106–122. <https://doi.org/10.1016/j.coastaleng.2017.08.004>.
- Toimil, A., Losada, I.J., Nicholls, R.J., Dalrymple, R.A., Stive, M.J.F., 2020. Addressing the challenges of climate change risks and adaptation in coastal areas: a review. *Coast. Eng.* 156, 103611. <https://doi.org/10.1016/j.coastaleng.2019.103611>.
- UNEP/MAP/PAP, 2008. Protocol on integrated coastal zone management in the mediterranean. Split. Prior. Actions Programm. ISBN: 978-953-6429-60-8 [https://pa.prac.org/storage/app/media/Dokumenti/Protocol\\_publicacija\\_May09.pdf](https://pa.prac.org/storage/app/media/Dokumenti/Protocol_publicacija_May09.pdf).
- Vitousek, S., Barnard, P.L., Limber, P., Erikson, L., Cole, B., 2017. A model integrating longshore and cross-shore processes for predicting long-term shoreline response to climate change. *J. Geophys. Res.: Earth Surf.* 122, 782–806. <https://doi.org/10.1002/2016JF004065>.
- Vitousek, S., Vos, K., Splinter, K.D., Erikson, L., Barnard, P.L., 2023. A model integrating satellite-derived shoreline observations for predicting fine-scale shoreline response to waves and sea-level rise across large coastal regions. *J. Geophys. Res.: Earth Surf.* 128. <https://doi.org/10.1038/s41598-024-77030-4> e2022JF006936.
- Voudoukas, M.I., Ranasinghe, R., Mentaschi, L., Plomaritis, T.A., Athanasiou, P., Luijendijk, A., Feyen, L., 2020. Sandy coastlines under threat of erosion. *Nat. Clim. Change* 10, 260–263. <https://doi.org/10.1038/s41558-020-0697-0>.
- Wainwright, D.J., Ranasinghe, R., Callaghan, D.P., et al., 2015. Moving from deterministic towards probabilistic coastal hazard and risk assessment: development of a modelling framework and application to Narrabeen Beach, New South Wales, Australia. *Coast. Eng.* 96, 92–99. <https://doi.org/10.1016/j.coastaleng.2014.11.009>.
- Wang, X., Dastgheib, A., Reyns, J., et al., 2024. An assessment of the tipping point behavior for shoreline retreat: a PCR model application at Vung Tau beach, Vietnam. *J. Mar. Sci. Eng.* 12, 2141. <https://doi.org/10.3390/jmse12122141>.
- Zhang, K.Q., Douglas, B.C., Leatherman, S.P., 2004. Global warming and coastal erosion. *Clim. Change* 64, 41–58. <https://doi.org/10.1023/B:CLIM.0000024690.32682.48>.